Discovery of 8-azabicyclo[3.2.1]octan-3-yloxy-benzamides as selective antagonists of the kappa opioid receptor. Part 1

Todd A. Brugel *, Reed W. Smith, Michael Balestra, Christopher Becker, Thalia Daniels, Tiffany N. Hoerter, Gerard M. Koether, Scott R. Throner, Laura M. Panko, James J. Folmer, Joseph Cacciola, Angela M. Hunter, Ruifeng Liu, Philip D. Edwards, Dean G. Brown, John Gordon, Norman C. Ledonne, Mark Pietras, Patricia Schroeder, Linda A. Sygowski, Lee T. Hirata, Anna Zacco, Matthew F. Peters

CNS Discovery Research, AstraZeneca Pharmaceuticals, 1800 Concord Pike, Wilmington, DE 19850, USA

ABSTRACT

Initial high throughput screening efforts identified highly potent and selective kappa opioid receptor antagonist 3 (κ IC$_{50}$ = 77 nM; μ:κ and δ:κ IC$_{50}$ ratios >400) which lacked CNS exposure in vivo. Modification of this scaffold resulted in development of a series of 8-azabicyclo[3.2.1]octan-3-yloxy-benzamides showing potent and selectivity κ antagonism as well as good brain exposure. Analog 6c (κ IC$_{50}$ = 20 nM; μ:κ = 36, δ:κ = 415) was also shown to reverse κ-agonist induced rat diuresis in vivo.

© 2010 Published by Elsevier Ltd.

Major depressive disorder (MDD), or depression, is a debilitating disease which effects anywhere from 8% to 10% of the global population.[1] The first line of treatment for those diagnosed with depression is often selective serotonin reuptake inhibitors (SSRIs) such as fluoxetine and escitalopram; however, 60% of patients treated with these medications fail to achieve remission.[2] Therefore, new methods of treatment that work through alternative mechanisms are of great interest to the medical and pharmaceutical community.

Kappa (κ) opioid receptors belong to a family of G-protein coupled receptors (GPCRs) which include mu (μ), delta (δ) and the opioid-like receptor (ORL-1). Historically, interest in the opioids has focused on agonists for analgesia. Recent and accumulating evidence indicates that two κ antagonists: nor-BNI 1[3] and JDTic 2[4] (Fig. 1), have anxiolytic and anti-depressant-like activity in rodents.[5] This role for κ in modulating mood appears to be conserved since κ agonists have profound depressant activity in humans.[6]

As part of our strategy to develop new small molecule treatments for depression, we initiated a program to identify selective and brain penetrant κ antagonists. We initiated a multifaceted campaign to screen our corporate compound collection using both novel virtual screening methods as well as an array of biological assays to identify

κ preferring antagonists that interacted in either an orthosteric or allosteric manner. Initially, we identified a series of potent and highly selective bis-amide alkoxypiperidines represented by compound 3 (Fig. 2). Unfortunately, these compounds showed poor in vitro permeability (MDCK-MDR1 $P_{app}A > B$ = <10 nm/s) resulting in minimal brain exposure (data not shown).

Realizing that the high MW of these compounds (>500 Da) could limit permeability, we investigated the effects of truncating this scaffold in an attempt to identify the most critical pharmacophore
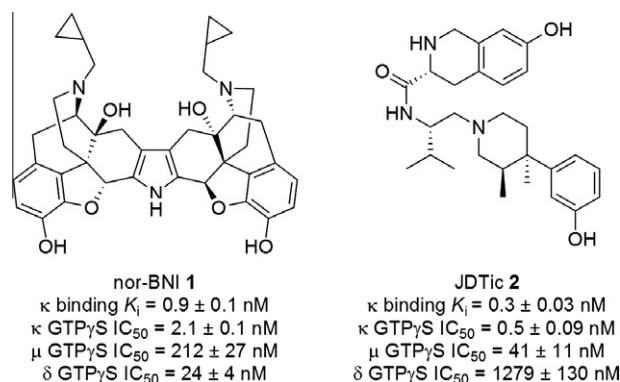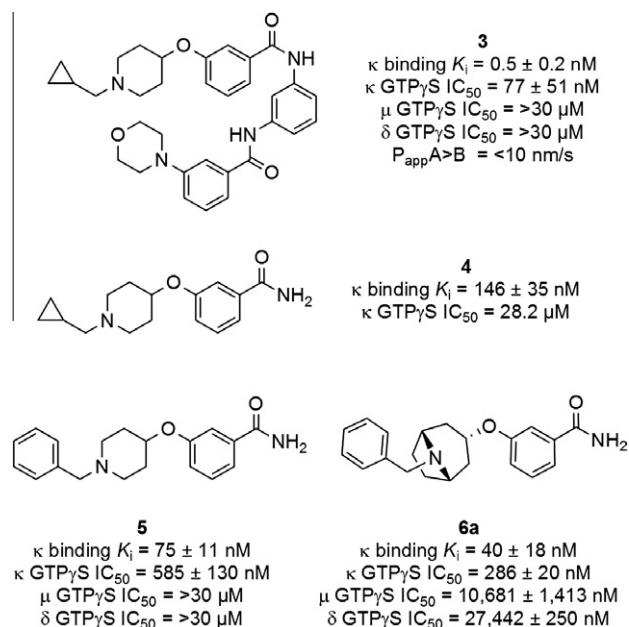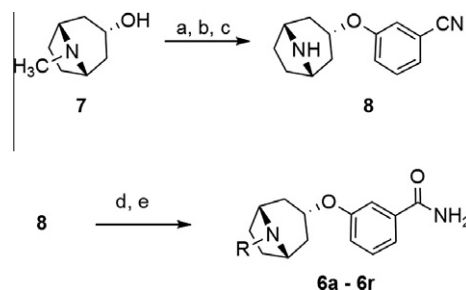

nor-BNI 1
κ binding K_i = 0.9 ± 0.1 nM
κ GTPγS IC$_{50}$ = 2.1 ± 0.1 nM
μ GTPγS IC$_{50}$ = 212 ± 27 nM
δ GTPγS IC$_{50}$ = 24 ± 4 nM

JDTic 2
κ binding K_i = 0.3 ± 0.03 nM
κ GTPγS IC$_{50}$ = 0.5 ± 0.09 nM
μ GTPγS IC$_{50}$ = 41 ± 11 nM
δ GTPγS IC$_{50}$ = 1279 ± 130 nM

Figure 1. Selective kappa opioid antagonists nor-BNI 1 and JDTic 2 (in-house data).

3
κ binding K_i = 0.5 ± 0.2 nM
κ GTPγS IC$_{50}$ = 77 ± 51 nM
μ GTPγS IC$_{50}$ = >30 μM
δ GTPγS IC$_{50}$ = >30 μM
P_{app}A>B = <10 nm/s

4
κ binding K_i = 146 ± 35 nM
κ GTPγS IC$_{50}$ = 28.2 μM

5
κ binding K_i = 75 ± 11 nM
κ GTPγS IC$_{50}$ = 585 ± 130 nM
μ GTPγS IC$_{50}$ = >30 μM
δ GTPγS IC$_{50}$ = >30 μM

6a
κ binding K_i = 40 ± 18 nM
κ GTPγS IC$_{50}$ = 286 ± 20 nM
μ GTPγS IC$_{50}$ = 10,681 ± 1,413 nM
δ GTPγS IC$_{50}$ = 27,442 ± 250 nM

Figure 2. 4-Alkoxypiperidine derived kappa opioid antagonists.
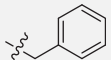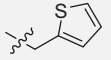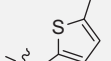
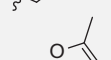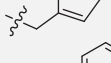**Scheme 1.** Reagents and conditions: (a) NaH, 3-fluorobenzonitrile, THF, 0–50 °C, 73%; (b) (i) ACE-Cl, DCM, reflux; (ii) MeOH, reflux; (iii) Boc$_2$O, THF/H$_2$O (1:1), NaHCO$_3$ (s), rt, 74%; (c) satd HCl/dioxane, dioxane, rt, 93%; (d) RCHO, DCM, NaBH(OAc)$_3$, rt; (e) KOH, t-BuOH, 80 °C.
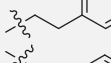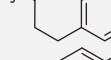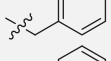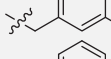
features. When the *meta*-piperidin-4-yloxybenzamide sub-unit **4** was tested, we observed near complete loss of κ antagonism as measured using a [^{35}S]GTPγS binding assay. Upon replacing the N-cyclopropylmethyl substituent with a benzyl (**5**, Fig. 2), we regained a significant amount of κ potency (κ IC$_{50}$ = 923 nM) while still maintaining excellent selectivity versus μ and δ (μ and δ IC$_{50}$ >30 μM). Additional modification to include an 8-azabicyclo[3.2.1]octane core (**6**) provided further enhancement of κ antagonism and selec-

Table 1
N-substitution opioid antagonist SAR for 3-oxo-*meta*-benzamide-8-azabicyclo-[3.2.1]-octanes **6a**–**6i**
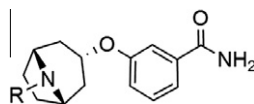
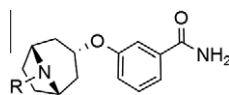| Compd	R	[^{35}S]GTPγS IC$_{50}$ (nM)			hERG IC$_{50}$[d] (μM)
		κ[a]	μ[b]	δ[c]	
6a		286 ± 20	10,681 ± 1413	27,442 ± 250	0.61
6b		215 ± 5	9359 ± 2275	>30,000	0.43
6c		20 ± 3	722 ± 47	8306 ± 1635	0.26
6d		386 ± 22	10,854 ± 2630	22,049 ± 150	2.8
6e		754 ± 292	424 ± 23	2145 ± 195	0.38
6f		342 ± 11	659 ± 74	4000 ± 900	0.25
6g		49 ± 2	482 ± 112	10,914 ± 2660	0.14
6h		148 ± 3	2648 ± 40	11,076 ± 300	0.52
6i		620 ± 356	17,554	>30,000	0.62

[a] Kappa (κ) antagonism was determined in a human [^{35}S]GTPγS assay using Dynorphin A(1–13) as the agonist stimulus. IC$_{50}$'s are reported as the mean ± SEM ($n \geqslant 2$) and without SEM where n = 1.

[b] Mu (μ) antagonism was determined in a human [^{35}S]GTPγS assay using DAMGO as the agonist stimulus. IC$_{50}$'s are reported as the mean ± SEM ($n \geqslant 2$) and without SEM where n = 1.

[c] Delta (δ) antagonism was determined in a human [^{35}S]GTPγS assay using SNC-80 as the agonist stimulus. IC$_{50}$'s are reported as the mean ± SEM ($n \geqslant 2$) and without SEM where n = 1.

[d] Inhibition of the human ether-a-go-go (hERG) voltage-gated ion-channel was determined using an IonWorks™ electrophysiology assay.[9] IC$_{50}$'s are reported as the mean of $n \geqslant 2$ experiments.

Table 2
N-substitution opioid antagonist SAR for 3-oxo-*meta*-benzamide-8-azabicyclo-[3.2.1]-octanes **6j–6t**

Compd	R	[^{35}S]GTPγS IC$_{50}$ (nM)			hERG IC$_{50}$ (µM)
		κ	µ	δ	
6j		241 ± 103	7854 ± 135	>24,727	1.5
6k		431 ± 133	2894 ± 1325	>21,889	3.5
6l		3159 ± 1735	19,001 ± 900	>30,000	1.9
6m	-CH$_3$	12,589	ND[a]	ND[a]	>33
6n		6691 ± 255	>30,000	>30,000	7.3
6o		204 ± 70	1826 ± 875	>30,000	2.0
6p		11 ± 1	307 ± 17	4842	0.62
6q	CH$_3$SO$_2$	39 ± 5	576 ± 39	5389 ± 590	6.6
6r		524 ± 54	9432 ± 3900	>27,287	>33
6s		3411 ± 540	21,090 ± 1950	>30,000	>33
6t		345 ± 36	253 ± 21	2668 ± 275	0.72

[a] ND = not determined.

tivity. In the discussion that follows, we describe the synthesis and emerging SAR of analogs of **6**, as well as highlight additional in vitro and in vivo properties.

Synthesis of 3-oxo-*meta*-benzamide-8-azabicyclo-[3.2.1]-octanes **6** commenced with S$_N$Ar addition of tropine **7** to 3-fluorobenzonitrile (Scheme 1). This was followed by demethylation using 1-chloroethyl chloroformate (ACE-Cl) to give crude NH tropane **8** after methanol mediated deprotection of the intermediate carbamate. To facilitate separation of the demethylated product from unreacted starting material, the crude material was treated with Boc$_2$O and the respective *t*-butyl carbamate was isolated via column chromatography. Deprotection with HCl/dioxane furnished pure **8**. Reductive amination of **8** with various aldehydes, followed by hydration of the nitrile to the primary benzamide provided N-substituted-azabicyclooctanes **6a–6r**.[7]

Final compounds were tested for their ability to inhibit agonist-stimulated activation of G-proteins using a [^{35}S]GTPγS binding assay in HEK membranes containing each of the cloned human opioid receptor subtypes.[8] Table 1 displays the results for a set of azabicyclooctanes containing various lipophilic aromatic N-substitutions. In addition to benzyl analog **6a**, unsubstituted 2-thiophene **6b** showed nearly identical potency and opioid selectivity. When the thiophene group was substituted with a methyl group at the 5-position (**6c**) we observed a 10-fold improvement in κ antagonism (IC$_{50}$ = 20 nM) without any loss in µ (µ:κ ratio = 36) or δ

(δ:κ ratio = 415) opioid selectivity. A similar trend was seen with 5-methyl-2-furanyl derivative **6d**. When attempting to extend the aromatic component further from the basic nitrogen with phenethyl analog **6e** and phenylpropyl analog **6f**, we saw moderate κ antagonism, but significant reduction in µ and δ selectivity ratios. The effect of different substitution patterns on the benzyl ring system was investigated with tolylmethyl analogs **6g–6i**.

Analog **6g** containing a *para*-tolylmethyl N-substitution showed the greatest κ antagonist potency, while the *ortho*-tolylmethyl analog **6i** was weakest. Conversely, the µ/κ selectivity followed the opposite trend with **6i** showing greater selectivity (µ:κ ratio = 28) compared to **6g** (µ:κ ratio = 10).

Although good levels of κ antagonism and opioid selectivity were achieved with this early set of analogs, we were aware of the potent hERG inhibition observed with many of these deriva-
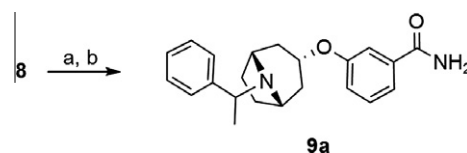
Scheme 2. Reagents and conditions: (a) (i) Ti(O-*i*-Pr)$_4$, acetophenone, 75 °C, 6 h; (ii) NaBH$_4$, EtOH; (b) KOH, *t*-BuOH, 80 °C.

tives. Sub-micromolar hERG potencies were found for all but one of these initial analogs (Table 1). In order to address this issue, we synthesized additional analogs which contained less lipophilic aromatic and non-aromatic N-substitutions. A subset of these compounds is highlighted in Table 2.

Incorporation of a 4- or 3-pyridylmethyl group (6j and 6k, respectively) was well tolerated and showed a modest improvement in hERG selectivity. Conversely, the 2-pyridylmethyl derivative 6l showed a 10-fold decrease in κ activity versus the parent benzyl derivative 6a. While smaller alkyl substituents like methyl (6m) and cyclopropylmethyl (6n) were weakly potent, the more hydrophobic cyclohexylmethyl derivative 6o showed good κ antagonism with a slight reduction in hERG inhibition relative to its aromatic counterparts. Analogs 6p and 6q represent attempts to incorporate more hydrophilic substituents onto the benzyl ring. We found that benzodioxole 6p provided one of our more potent κ antagonists. Selectivity versus μ and δ was also high, but hERG inhibition remained sub-micromolar. The selectivity between κ and hERG was still higher (hERG:κ ratio = 56) than many of the more hydrophobic aromatic examples like 6c (hERG:κ ratio = 13). Even better results were seen with benzylmethylsulfone 6q which showed potent κ antagonism (IC$_{50}$ = 39 nM) as well as elevated hERG selectivity (hERG:κ ratio = 169). Pyrazolomethyl derivative 6r lacked any significant hERG inhibition, although κ antagonism became more moderate. Finally, several acetyl amide analogs were synthesized and tested. Tertiary amides such as 6s lacked hERG activity, but also suffered from poor κ antagonism. Potency at the κ receptor was recovered through incorporation of more hydrophobic amide substitutions as in 6t. Unfortunately, this also resulted in similar enhancement of the hERG potency.

With our success in finding several N-substitutions that could alleviate some of the safety concerns involving high hERG activity arose another potential issue regarding CNS penetration. For instance, pyrazole 6r which showed one of the better κ:hERG ratios, proved to be a P-gp efflux substrate ($P_{app} B > A / P_{app} A > B$ ratio = 15) when tested in our in vitro MDCK-MDR1 permeability assay;
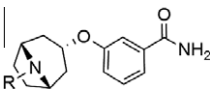
therefore, we became focused on identifying ways by which to reduce hERG inhibition without negatively effecting potential brain exposure.
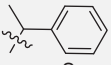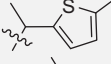
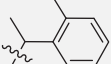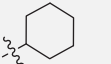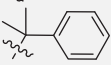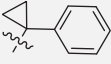During one phase of our SAR exploration of the azabicyclooctane nitrogen substitution, we looked at effects of branching at the α-position of the N-substituent. The synthesis of these derivatives required reductive amination between intermediate 8 and a ketone. This was done through initial formation of the iminium ion using titanium isopropoxide, followed by in situ reduction with sodium borohydride.[10] Subsequent hydration of the nitrile using standard conditions furnished α-methyl-branched analogs such as 9a (Scheme 2).

Table 3 displays the in vitro results for a set of α-branched analogs 9a–9g. Compared to their des-methyl counterparts 6a, 6c, and 6i, branched derivatives 9a–9c showed a 3.5, 18 and 1.3-fold loss in κ potency, respectively; however, this was in concurrence with a 9.8, 6.1 and 7.9-fold reduction in hERG inhibition, respectively. This was accomplished while maintaining the P-gp efflux ratio below 2 for these branched analogs. Tetralone derived compound 9d which fused the branched substituent to the benzyl ring showed even further degradation of κ antagonism while maintaining sub-micromolar hERG activity. Cyclohexyl derivative 9e showed similar potency to 9a and showed a reduced hERG IC$_{50}$ of 15 μM. Unfortunately, we noticed an increase in the P-gp efflux ratio of this compound to 9.5, which lessened further interest in this modification. Finally, quaternary substitution at the α-position was explored with gem-dimethyl analog 9f and spirocyclopropane 9g which were synthesized in part through a modified Robinson tropanone synthesis.[11] This change to an achiral substitution pattern resulted in near total loss of κ antagonism.

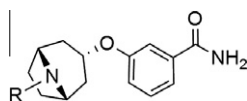We proceeded to study the profile of individual enantiomers of various α-methyl-branched analogs. Racemic α-methyl-4-pyridylmethyl analog 9h showed only modest κ antagonism and hERG inhibition (Table 4). Upon separation of 9h into its individual (R)-9i and (S)-9j enantiomers by chiral supercritical fluid chromatography (SFC), a trend appeared.[12] The more potent enantiomer 9i also

Table 3
SAR for racemic and achiral α-branched 3-oxo-meta-benzamide-8-azabicyclo-[3.2.1]-octanes analogs 9a–9g

Compd	R	[^{35}S]GTPγS IC$_{50}$ (nM)		hERG IC$_{50}$ (μM)	Efflux ratio[a]
		κ	μ		
9a		1003 ± 46	19,837 ± 3200	6.0	1.4
9b		355 ± 65	8504 ± 1120	1.6	1.9
9c		846 ± 13	16,785 ± 200	4.9	1.1
9d		2193 ± 195	22,696 ± 700	0.95	1.7
9e		1126 ± 188	9410 ± 3695	15	9.5
9f		13,266 ± 400	ND[a]	4.7	1.6
9g		24,234 ± 2900	>30,000	4.8	1.9

[a] Efflux is measured as a ratio of transport from apical to basolateral (A > B) versus basolateral to apical (B > A) directions using stably expressed human multidrug-resistant (MDR1) P-glycoprotein (P-gp) expressed MDCK cells.

Table 4
SAR for racemic and chiral α-branched 3-oxo-*meta*-benzamide-8-azabicyclo-[3.2.1]-octanes analogs **9h–9o**

Compd	R	[³⁵S]GTPγS IC$_{50}$ (nM)		hERG IC$_{50}$ (μM)	Efflux ratio
		κ	μ		
9h		1410 ± 300	>30,000	3.7	1.4
9i		683 ± 18	>24,383	13	1.9
9j		20,502 ± 3350	>30,000	1.8	1.1
9k		111 ± 16	2698 ± 125	2.8	1.7
9l		46 ± 5	1046 ± 125	4.6	9.5
9m		130 ± 2	1896 ± 205	3.0	1.6
9n		307 ± 82	22,931 ± 4200	13	1.9
9o		90 ± 11	1944 ± 105	3.3	3.3

showed a greater decrease in hERG inhibition relative to the racemate **9h**. Based on this result, several additional enantiomer pairs were separated. Data for the most potent enantiomers **9k–9o** are presented in Table 4.[13] In all cases, the selectivity between κ and hERG was greatly improved relative to that which was observed with the racemates or with the various non-α-branched analogs described in Tables 1 and 2. Particularly noteworthy was *meta*-methoxy-α-methylbenzyl derivative **9l** which showed potent κ antagonism (IC$_{50}$ = 46 nM) and a large hERG:κ ratio of 100. Additionally, selectivity versus μ was 23-fold and the P-gp efflux ratio <2.

A pharmacophore model for κ was developed in-house using several known potent and selective κ antagonists.[14] N-5-Methyl-thiophene analog **6c** was aligned to this model in order to generate a plausible binding orientation. Figure 3 represents the results of an overlay of low energy conformations of **6c** and nor-BNI **1** in the pharmacophore model. The Asp$_{138}$ and His$_{293}$ residues comprise the conserved region of opioid receptors referred to as the 'message'. The Glu$_{297}$ residue has been termed part of the 'address' region of κ, conveying selectivity for kappa over the other opioid subtypes.[15] Analog **6c** and **1** are proposed to make salt-bridge interactions with the Asp$_{138}$ and Glu$_{297}$ residues of κ. nor-BNI makes additional interactions with the receptor including the His$_{293}$ residue in this model, which may explain, in part, its greater potency.

Table 5 summarizes the in vitro ADME profile for a set of diverse κ antagonists. Overall, most analogs in this series proved to be metabolically stable in human liver microsomes. Analogs **6c** and **6o** showed higher rat microsomal instability, while the pyridine analog **9m** proved to be more stable. Permeability (MDCK-MDR1 $P_{app}A > B$) and P-gp efflux ratios were seen as very good for **6c** and **6o**, while the α-branched analog **9m** showed moderate permeability but with an increased P-gp efflux ratio compared to the other two analogs. All three representatives showed high unbound levels of compound as measures in rat plasma protein binding (PPB).

We followed up our in vitro evaluation of select compounds in this series with in vivo pharmacokinetic and/or CNS exposure studies in the rat. As summarized in Table 6, when dosed intravenously, analogs **6c** and **6o** showed high plasma clearance and moderate volumes of distribution (VD$_{ss}$) resulting in the observed short half-lives. CNS exposure was observed to be high for both analogs, with measured brain/plasma concentration ratios ([Br]/[Pl]) near two-fold. The poor bioavailability (% F) seen for these compounds was consistent with the observed high in vitro first pass clearance, as evidenced by the high Cl$_{int}$ observed in rat liver microsomes.
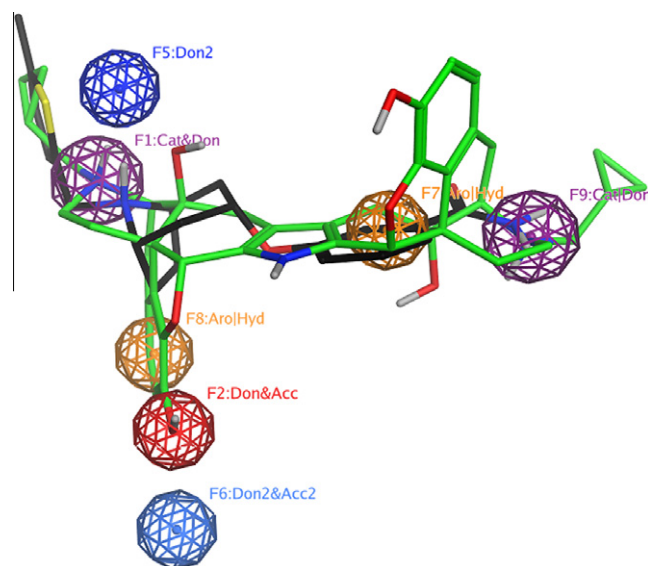
Figure 3. Overlay of nor-BNI **1** (green carbons) and **6c** (black carbons) in pharmacophore model of the kappa opioid receptor binding site.

Table 5
In vitro DMPK properties for azabicyclo[3.2.1]octane derivatives **6c**, **6o** and **9m**

Compd	κ IC_{50} (nM)	hCL_{int}[a]	rCL_{int}[a]	P_{app} $A > B$[b]	Efflux ratio[c]	Rat PPB (% free)[d]
6c	20	31	379	130	1.4	50
6o	204	<4	196	83	2.6	46
9m	130	<4	14	91	4.0	81

[a] Human and rat liver microsomal intrinsic clearance (hCL_{int}) was measured as μl/min/mg protein according to the standard liver microsomal stability assay protocol.
[b] P_{app} $A > B$ is the rate (nm/s) of transport in the apical to basolateral ($A > B$) direction as measured across the MDR1-MDCK cell monolayer stably expressing the human multidrug-resistant (MDR1) protein, P-glycoprotein.
[c] See footnote a from Table 3 for efflux assay description.
[d] Rat plasma protein binding (PPB) was determined as percent free (% free) compound available after incubation in male Sprague-Dawley rat plasma.

Table 6
In vivo rat pharmacokinetic profile for azabicyclo[3.2.1]octane derivatives **6c** and **6o**

Compd	CL[a] (ml/min/kg)	$t_{1/2}$[a] (h)	VD_{ss}[a] (L/kg)	[Br]/[Pl][a]	% F[b]
6c	113	1.0	5.1	1.7	4
6o	184	1.0	9.5	1.8	5

[a] Plasma clearances (CL), half-lives ($t_{1/2}$), volume of distributions (VD_{ss}) and brain:plasma concentration ratios ([Br]/[Pl]) were measured after a 2 μmol/kg intravenous (iv) infusion dose in Sprague-Dawley rats.
[b] Percent bioavailability (% F) was measured using the above iv data along with data from a 2 μmol/kg (**6c**) or 6 μmol/kg (**6o**) oral (PO) dose in Sprague-Dawley rats.

Finally, the α-branched methylpyridine analog **9m** was found to possess moderate brain exposure (total brain/plasma ratio = 0.36 measured 2 h after a 5 μmol/kg iv infusion dose). This result was in agreement with the borderline permeability and P-gp efflux values observed in vitro.

For κ agonists that cross the blood–brain barrier, one of the prohibitive side effects is diuresis. Endogenous κ agonists do not appear to tonically regulate urine output since resting urine flow is not significantly altered by κ antagonists (unpublished in-house results). Antagonists do, however, reverse agonist-induced diuresis in rodents and this paradigm serves as a useful pharmacodynamic model for evaluating in vivo effects that are CNS-mediated.[16] Specifically, κ-selective agonist U50488 (2.5 mg/kg SC dose) induced diuresis was dose dependently reversed with κ antagonist **6c** (ID_{50} = 6 μmol/kg, p <0.01) as compared to administration of U50488 alone.[17]

In summary, our lead generation efforts have identified a new class of low molecular weight (<400 Da) κ antagonists based on an 8-azabicyclo[3.2.1]octan-3-yloxy-benzamide structure which show excellent in vitro potency and selectivity versus μ and δ opioid receptors. Initial concerns with significant hERG inhibition and high in vitro P-gp efflux were mitigated through modification of the pendant N-substitution. Several analogs, including **6c** and **6o**, showed good overall pharmacokinetic profiles. Methylthiophene analog **6c** also displayed in vivo activity in reversing κ agonist stimulated diuresis in rats.

Acknowledgements

Supplementary data

An experimental procedure detailing the preparation of **6c** via the route outlined in Scheme 1, as well as details pertaining to the opioid [^{35}S]GTPγS assay, VDC studies, pharmacophore modeling and the rat diuresis in vivo model. Supplementary data associated with this article can be found, in the online version, at doi:10.1016/j.bmcl.2010.07.113.

References and notes

1. Kessler, R. C.; Berglund, P.; Demler, O. *JAMA* **2003**, *289*, 3095.
2. Trivedi, M. H.; Rush, A. J.; Wisniewski, S. R.; Nierenberg, A. A.; Warden, D.; Ritz, L.; Norquist, G.; Howland, R. H.; Lebowitz, B.; McGrath, P. J.; Shores-Wilson, K.; Biggs, M. M.; Balasubramani, G. K.; Fava, M. *Am. J. Psychiatry* **2006**, *163*, 28.
3. Portoghese, P. S.; Nagase, H.; Lipkowski, A. W.; Larson, D. L.; Takemori, A. E. *J. Med. Chem.* **1988**, *31*, 836.
4. Thomas, J. B.; Atkinson, R. N.; Rothman, R. B.; Fix, S. E.; Mascarella, S. W.; Vinson, N. A.; Xu, H.; Dersch, C. M.; Lu, Y.; Cantrell, B. E.; Zimmerman, D. M.; Carroll, F. I. *J. Med. Chem.* **2001**, *44*, 2687.
5. (a) Nague, S. D.; Pliakas, A. M.; Todtenkopg, M. S.; Tomasiewicz, H. C.; Zhang, Y.; Stevens, W. C., Jr.; Jones, R. M.; Portoghese, P. S.; Carlezon, W. A., Jr. *J. Pharmacol. Exp. Ther.* **2003**, *305*, 323; (b) McLaughlin, J. P.; Maron-Popovici, M.; Chavkin, C. *J. Neurosci.* **2003**, *23*, 5674; (c) Knoll, A. T.; Meloni, E. G.; Thomas, J. B.; Carroll, F. I.; Carlezon, W. A. *J. Pharmacol. Exp. Ther.* **2007**, *323*, 838.
6. Carlezon, W. A., Jr.; Beguin, C.; DiNieri, J. A.; Baumann, M. H.; Richards, M. R.; Todtenkopf, M. S.; Rothman, R. B.; Ma, Z.; Lee, D. Y.; Cohen, B. M. *J. Pharmacol. Exp. Ther.* **2006**, *316*, 440.
7. All new analogs were synthesized in >95% purity as determined by ^{1}H NMR and LCMS analysis.
8. Measured [^{35}S]GTPγS EC_{50}'s for κ and μ functional agonism for select compounds in this report were all >30 μM.
9. Schroeder, K.; Neagle, B.; Trezise, D. J.; Worley, J. *J. Biomol. Screening* **2003**, *8*, 50.
10. Bhattacharyya, S. *Tetrahedron Lett.* **1994**, *35*, 2401.
11. (a) Robinson, R. *J. Chem. Soc., Trans.* **1917**, *111*, 762; (b) Suzuki, M.; Ohuchi, Y.; Asanuma, H.; Kaneko, T.; Yokomori, S.; Ito, C.; Isobe, Y.; Uramatsu, M. *Chem. Pharm. Bull.* **2001**, *49*, 29.
12. Absolute configurations of **9i**, **9j** and **9l** were determined using vibrational circular dichroism (VCD). For a review of VCD see: Nodie, L. A.; Dukor, R. K. In *Applications of Vibrational Spectroscopy in Pharmaceutical Research and Development*; Pivonka, D. E., Chalmers, J. M., Griffiths, P. R., Eds.; John Wiley: Chichester, 2007; pp 129–154.
13. Absolute configuration assignments based on GTPγS data in conjunction with VCD results for **9i**, **9j** and **9l**.
14. See the Supplementary data section for a method description for the κ pharmacophore model.
15. Metzger, T. G.; Paterlini, M. G.; Portoghese, P. S.; Ferguson, D. M. *Neurochem. Res.* **1996**, *21*, 1287.
16. Gottlieb, H. B.; Varner, K. J.; Kenigs, V. A.; Cabral, A. M.; Kapusta, D. R. *J. Pharmacol. Exp. Ther.* **2005**, *312*, 678.
17. See the Supplementary data section for a detailed description of the diuresis results for **6c**. A companion manuscript describing efficacy in an anxiety/depression-like animal model for **6c** (termed **MTAB**) is in preparation (Peters, M.F. et al.).